Volume 13, Number 6, November 1993 ISSN 0890-4332

Title Page, Volume Contents and Author Index for Volume 13 are bound in at the back of this issue

HEAT RECOVERY SYSTEMS & CHP

combined heat & power

Editor-in-Chief: D.A. REAY

Special Issue

Process Intensification

Guest Editor: P. A. Pilavachi

PERGAMON PRESS

OXFORD · NEW YORK · SEOUL · TOKYO

Heat Recovery Systems & CHP Vol. 13, No. 6, pp. 547–563, 1993
Printed in Great Britain

0890-4332/93 $6.00 + .00
Pergamon Press Ltd

HEAT TRANSFER ENHANCEMENT WITH CONDENSATION BY SURFACE ROTATION

L. L. VASILIEV and V. V. KHROLENOK
A. V. Luikov Heat and Mass Transfer Institute, P. Brovka, 15, 220728, Minsk, Byelorussia

(*Received* 5 *February* 1992)

Abstract—Process intensification relies on many unit operations on enhanced heat transfer. One technique for the enhancement of condensation heat transfer is the use of surface rotation. This is particularly effective in reducing the condensate film thickness.

The formulae and relationships given in this paper are concerned with rotating discs and tubes, and can be used for developing advanced heat exchanger concepts.

NOMENCLATURE

b	groove width
D, d	diameter
f_v	friction coefficient
G	mass flow rate
G_1	specific volume flow rate
g_o	gravitational acceleration;
L, l	length
n	number of grooves
P	pressure
Q	heat flux
q	heat flux density
R, r	radius
r^*	latent heat of vaporization
S_s	shear stress at the fluid–vapour interface

Greek letters

λ	thermal conductivity
α	heat transfer coefficient
ρ	density
μ	dynamic viscosity coefficient
ν	kinematic viscosity coefficient
$\eta = \omega^2 R/g_0$	overload
δ	fluid layer thickness
φ	half opening angle of cone
τ	shear stress
v, w	linear velocity
$Nu = \alpha l/\lambda$, $Nu_A = \alpha D/\lambda$	Nusselt number
$P_\tau = \nu c_p \rho/\lambda$	Prandtl number
$Re = 4G_1/\nu = 4v\delta/\nu = 4qL/(\rho \nu r^*)$	
$Re_r = \omega R^2/\nu$, $Re = \omega\delta^2/\nu$	Reynolds number
$Ga = \omega^2 Rl^3/\nu^2$, $Ga_R = \omega^2 R^4/\nu^2$	Galileo number
$We = \rho\omega^2 D^3/(4\sigma g_o)$	Weber number
$Ca = \omega R\mu/\sigma$	
$Ku = r^*/(c_p \Delta T)$	
$Fr_c = \eta = \omega^2 R/g_0$	
$A = \sigma^*/R$	
$\sigma^* = [\sigma/(\rho g_o)]^{1/2}$	

Subscripts

f	fluid
v	vapour
m	minimum
c	condensation surface
op	optimal

1. INTRODUCTION

Heat transfer with condensation on a cooled surface is realized in numerous engineering facilities. Heat transfer enhancement in modern technical devices could be provided by different techniques particularly using so called active and passive enhancement methods (gravity, electrohydrodynamics, ultrasonic, capillary forces, rotation) and combinations thereof. Heat transfer enhancement with condensation in rotating devices such as discs, tubes, heat pipes, drums, rotors, bearing, etc. is efficient when the process intensification takes place on the external and internal surfaces of heat transfer. For example the external heat transfer is provided by water-sprayed finned surfaces and high velocities of rotation. Internal heat transfer is guaranteed by heat transfer with condensation in rotating condensers, where the condensation heat transfer coefficient is proportional to the angular velocity to the 2/5ths power.

When the film condensation occurs inside tubes or discs the main thermal resistance depends on the liquid film thickness. Rotation of condensers is one of the ways to decrease liquid film thickness and to provide a significant degree of enhancement of heat and mass transfer. The centrifugal forces may be several times greater than the gravity or capillary forces or comparable with them. Therefore, it is promising to use some combinations of these forces to guarantee a high rate of heat transfer in a large variety of angular velocities of rotation. Condensate flow dynamics are affected by surface orientation in space, condenser geometry, surface position relative to the rotation axis, proportion between gravity, centrifugal and capillary forces, interaction of liquid and vapour flows, etc. Nowadays, many researchers seek to advance our fundamental understanding of film condensation on enhanced surfaces. In particular, they are concerned with the development of a theoretical model to predict the heat transfer coefficient as a function of fluid properties, surface geometry and velocity of rotation.

Condensation on enhanced surfaces in the presence of centrifugal, gravity and capillary forces allows significant energy saving, relative to plain surfaces. Also, although several analytically based models have been proposed, they are quite inadequate, because the mechanism of condensation on enhanced surfaces is not completely understood. The current lack of predictive ability severely inhibits their introduction to new process fluids and engineering applications.

2. CONDENSATION ON ROTATING DISCS

Rotating discs as heat transfer surfaces with condensation on one side are used to increase the heat transfer coefficient during water distillation, liquid heat treatment [1–3] and so on.

A theoretical analysis of vapour condensation on a rotating horizontal disc was first made in ref. [4]. Inertia forces and convective heat transfer were taken into account, other assumptions made by the authors are similar to those by Nusselt [4] for condensation of a practically immovable vapour on a vertical surface. To calculate heat transfer for ordinary liquids ($Pr \geqslant 1$) at small $c_p \Delta T/r^*$, the formula

$$\frac{\alpha(\nu/\omega)^{0.5}}{\lambda} = 0.904\left(\frac{Pr}{c_p \Delta T/r^*}\right)^{0.25}, \tag{1}$$

was obtained, where $\Delta T = T_v - T_w$ is the difference between a saturated vapour and wall temperature.

With the assumptions made in [4], an analysis of film condensation on a rotating disc with constant heat supply was made in [5]. The following formula was derived for the calculation of heat transfer

$$\alpha = 0.874\left(\frac{\rho\omega^2 r^* \lambda^3}{\nu q}\right)^{1/3}. \tag{2}$$

Comparison of equations (1) and (2) shows that these formulae are identical. Therefore, heat transfer with vapour condensation on a rotating disc does not depend on disc radius, i.e. local mean α values should be equal.

Heat transfer with vapour condensation on a rotating disc was studied experimentally in refs [6–12]. The experimental heat transfer values obtained in [6, 9] are 45–50% less than those

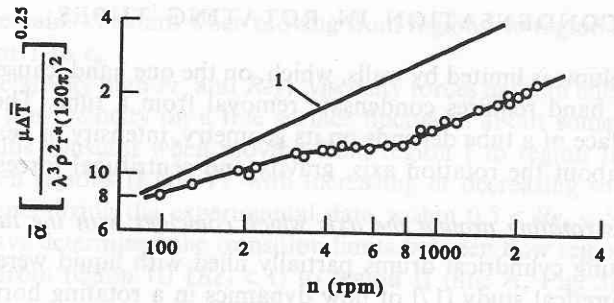

Fig. 1.

calculated by equation (1). In [7], the heat transfer coefficients close to the values predicted by (1) were obtained for $\omega > 53\ s^{-1}$, while for $\omega < 53\ s^{-1}$, the experimental data are essentially in excess of the predicted ones. The data obtained in [10] are characterized by essential scatter, the mean heat transfer coefficients being 25–40% lower than those calculated by equation (1). The experiments [10] on vapour condensation on the rotating disc surface turned down (Fig. 1) have shown that at a constant disc rotational velocity, $\alpha \sim \Delta T^{0.25}$. The α dependence on ω for $\overline{\Delta T} = \text{const}$ can be split into two segments: the first, from 10 to 40–50 s^{-1}, and the second, above 52 s^{-1}. For the first segment, $\alpha \sim \omega^{0.23}$; for the second, $\alpha \sim \omega^{0.5}$. The authors explain the smaller ω effect on the heat transfer rate within the first section by the fact that at low rotational velocities within the disc sections close to the rotation centre, the flow is affected by the gravity forces which separate droplets from the film. Within the second section, heat transfer and liquid film flow are, mainly, determined by centrifugal forces. The authors [9] have observed similar condensate flow, and, for $\omega > 60\ s^{-1}$, have generalized the experimental heat transfer data by the formula

$$\bar{\alpha} = 1.18\left(\frac{\lambda^3\rho^2 r^*}{\mu\,\Delta T}\right)^{0.25}\omega^{0.43}. \tag{3}$$

In [11], vapour condensation on rotating discs with radial grooves was studied. The experimental data show up to a 65% increase in the heat transfer coefficient in the case of film condensation.

Heat transfer with vapour condensation from a vapour–air mixture on a rotating disc was studied in [12]. As shown, rotation of a heat transfer surface essentially (3–5 times) increases the mass transfer coefficient. The experimental results (Fig. 2) are described within ±15% by the equation

$$Nu_D = 2.23\ Re^{1/3}\pi_D^{-0.6}\epsilon_a^{-0.4}. \tag{4}$$

The basic parameters were: volume content of air, ϵ_a, from 0.004 to 0.5; $Re = (2.95\ldots115.2)\cdot10^3$; π_D from 0.05 to 0.73.

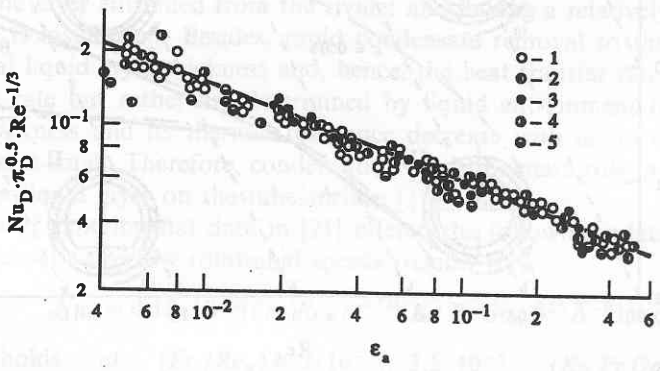

Fig. 2.

3. CONDENSATION IN ROTATING TUBES

Inside a tube, vapour volume is limited by walls, which, on the one hand, causes directed vapour motion and on the other hand requires condensate removal from a tube. The condensate film thickness on the inner surface of a tube depends on its geometry, intensity of heat transfer, spatial orientation and position about the rotation axis, gravity and centrifugal forces, etc.

3.1. *Condensation in tubes rotating around the axis which coincides with the tube symmetry axis*

Flow dynamics in rotating cylindrical drums partially filled with liquid were studied in many works [13–21], etc. A theoretical study [17] of flow dynamics in a rotating horizontal cylindrical tube cross section showed that they were determined by the following two dimensionless numbers: $Re_\delta = \omega\bar{\delta}^2/\nu$ and $Fr_c = \eta = \omega^2 R/g_0$. It depends both on the relationship between gravity and centrifugal forces and on physical properties and amount of the liquid (δ being the mean liquid layer thickness on the tube surface). Numerical solution of motion and the continuity equation for annular flows [17] provided velocity profiles in a liquid layer and the flow diagram is shown in Fig. 3.

Experimental studies [18] have proved the validity of theoretical results [17] for determining flow dynamics in a blind cylinder. Four flow regimes were found (Fig. 3): (I) solid body rotation; (II) entrained off thin layer; (III) viscous flow; and (IV) inertia flow. In regime II the flow pattern is characterized by a "rivulet" at the tube bottom; annular liquid distribution over the interior surface is observed for the three other regimes. The position of a free liquid surface is determined by two parameters: an angular coordinate of a maximum layer thickness, φ_m, and maximum-to-mean layer thickness ratio, $\epsilon = \delta_m/\bar{\delta}$. In regime I, liquid is uniformly distributed over the tube surface ($\epsilon \to 1$) and is moving at a constant angular velocity equal to the rotational velocity of the tube. This regime is observed at small Fr_c, when the liquid is viscous or in small amounts, and at large Fr_c. In the former case, viscosity forces are prevailing throughout the entire liquid layer thickness, while in the latter case, they are dominating only at the wall, in the boundary layer whose thickness decreases with increasing ω. Beyond the boundary layer, fluctuations are imposed on liquid motion, which are stipulated by the gravity force and have the amplitude tending to zero with increasing Fr_c.

In regime II, the tube bottom is filled by the rivulet, while the other surface is covered by a thin liquid layer. This regime is observed at small Fr_c or large Re_δ, i.e. for low liquid viscosity or a large amount of liquid. In this case, neither viscous nor inertia forces can provide liquid distribution over the tube surface without a rivulet. In regime III, viscous and gravity forces prevail over centrifugal forces. The velocity of film flowing down under gravity forces is compatible with the linear wall velocity. The Fr_c and Re_δ numbers are small. The angular position of the maximum layer thickness

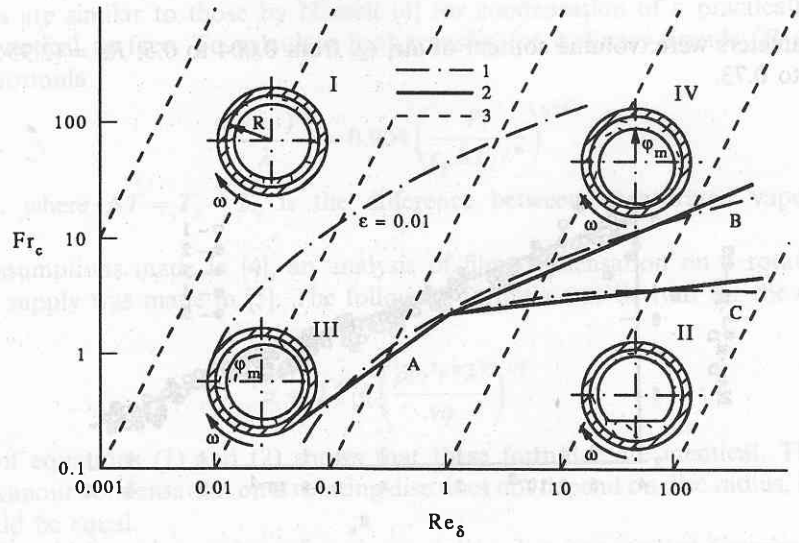

Fig. 3.

is $\varphi_m = \pi/2$ and remains constant when moving from region I to region II by changing the rotation frequency, ϵ, from 1 to ϵ_m.

In regime IV (relatively high Fr_c and Re_δ), viscosity forces have an effect only in a thin wall liquid layer. The liquid flow velocity on a free surface fluctuates about some mean value equal to ωR; $\varphi_m = 0$ and remains constant when moving from region I to region II; ϵ changes from 1 to ϵ_m. Transition between regions II and IV with increasing or decreasing rotation frequency occurs at different ω. In generalizing the experimental data within $0.5 < Re_\delta < 500$ and $0.2 < Fr_c < 50$, the authors of [18] have determined the transition limits between flow regions in a horizontal rotating cylindrical tube: from region III ($Re_\delta < 1$) to region II (line A, Fig. 3)

$$Fr_c = 2.2\, Re_\delta^{0.77}; \tag{5}$$

from region IV ($Re_\delta > 1$) to region III

$$Fr_c = 2.2 Re_\delta^{0.44} \tag{6}$$

with increasing rotation frequency (line B),

$$Fr_c = 2.2 Re_\delta^{0.13} \tag{7}$$

with decreasing rotation frequency (line C).

There is no clear boundary for region I, as the value of ϵ monotonically approaches unity as Fr_c increases. In Fig. 3, a conventional boundary of region I is shown to correspond to $\epsilon = 1.01$. At low tube rotation speeds, when the rivulet is present (region II), the liquid layer thickness, δ, beyond the rivulet is determined by its entrainment by a rotating cylindrical wall. In [21], a formula is derived to determine the entrained layer thickness depending on the angular velocity, tube radius, liquid physical properties and its amount:

$$\Delta_y = 2 \cdot 10^{-2} Ca^{0.68} (\bar{\Delta})^{0.36} \exp(11.8A). \tag{8}$$

This formula satisfactorily agrees with the authors' experimental data at $Ca < 0.01$. At $Ca > 0.01$ corresponding to large ω, the deviation of experimental from theoretical data is due to wave formation observed on the liquid surface.

At low rotation frequencies (region II), heat is transferred by vapour condensation on the surface of a thin liquid layer moving across the tube. The liquid is transported in a rivulet along the tube due to hydrostatic pressure. At high rotation frequencies (beyond region II) heat is transferred through an annular liquid layer pushed along the tube by hydrostatic pressure.

For regime II, the tube surface liquid layer thickness is determined by two processes: liquid entrainment from the rivulet and condensation. At rather a high angular velocity, the condensation is caught by the entrained liquid layer to be transported in the direction of tube rotation. As ω decreases, the moment occurs when a separation line appears on the ascending tube side, below which the condensate flows down into the rivulet in a counter-rotation mode. Above this line, it is entrained by the wall and gets into the "brook" moving in the direction of rotation. As the rotation speed decreases, the separation line moves upwards to take the position on the upper tube generation in a limited case at $\omega = 0$. At high ω in region II, the liquid increment due to condensation on the layer entrained from the rivulet and having a relatively large thickness and thermal resistance is insufficient. Besides, rapid condensate removal to the rivulet takes place. Therefore, the total liquid layer thickness and, hence, the heat transfer rate only weakly depend on the convection rate but rather are determined by liquid entrainment from the rivulet. The entrained layer thickness and its thermal resistance decrease with ω. In this case, the rate of condensate removal is small. Therefore, condensation plays the main role in the formation of the total thickness of a liquid layer on the tube surface [21].

A generalization of experimental data in [21] offered the following relation to calculate heat transfer with condensation at low rotational speeds (region II):

$$\overline{Nu}_R = 4.15 \cdot 10^{-2} (Fr_c/Re_R)^{-0.134} (Ku\, Pr\, Ga_R)^{0.25} \bar{\Delta}^{-0.1}. \tag{9}$$

This relation holds at $(Fr_c/Re_R) = 5 \cdot 10^{-7} \ldots 3.5 \cdot 10^{-5}$, $(Ku\, Pr\, Ga_R) = 4 \cdot 10^{11} \ldots 3 \cdot 10^{13}$, $\bar{\Delta} = 3 \cdot 10^{-3} \ldots 2.2 \cdot 10^{-2}$.

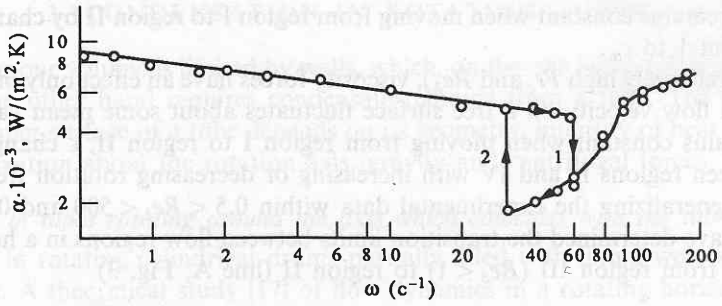

Fig. 4.

Heat transfer with condensation on an internal surface of a hollow horizontal cylinder for liquid flow region I (high rotation frequency) was discussed in many studies [18–30]. In this case, centrifugal forces are directed normal to the tube surface, liquid flow depends on the hydrostatic pressure and, hence, on the film thickness along the tube. Heat transfer may have a finite value if condensate flow down from the tube edges is possible.

For laminar film condensation on the surface normal to mass or inertia forces and with no shear stresses at the liquid–vapour interface (Fig. 5a), the following expressions are obtained in ref. [22] to calculate liquid film thickness:

$$X = \left(\frac{3}{2K_1}\frac{\delta_{\max}^5}{L^2}\right)^{1/2} I(\vartheta) \tag{10}$$

and heat transfer:

$$\overline{Nu} = \frac{\bar{\alpha}L}{\lambda} = \left[\left(\frac{2}{3}\right)^4 \frac{L^3}{K_1}\right]^{1/5} \frac{(1-\vartheta_{\min}^3)^{1/2}}{[I(\vartheta_{\min})]^{3/5}}, \tag{11}$$

where $K_1 = 3\lambda\mu\,\Delta T/(g\rho^2 r^*)$; $X = x/L$; $\vartheta = \delta/\delta_{\max}$; $I(\vartheta) = \int_\vartheta^1 \xi^3(1-\xi^3)^{-1/2}\,d\xi$, which can be integrated by parts and expressed in terms of the elliptical first kind integral as a function determined by standard tables. As shown, for $\vartheta_{\min}$ from 0 to 0.8, equation (11) can be described by an approximate formula with an error of not more than 1%:

$$\overline{Nu} = \left[\left(\frac{2}{3}\right)^4 \frac{L^3}{K_1}\right]^{1/5} [0.5 + 0.92(1-\vartheta_{\min}^3)^{1/2}]. \tag{12}$$

In ref. [23], it is shown that calculations by (12) give the heat transfer results weakly dependent on the exact flow down condition at $\vartheta_{\min} \leqslant 0.4$. For condensation on the internal hollow cylinder surface, assuming $g = \omega^2 R$, and $\vartheta_{\min} = 0$ and $\delta \ll R$, equation (12) can be represented in the form [24]:

$$\overline{Nu} = 0.824\left(\frac{\omega^2 R L^3}{\nu^2}\frac{Pr\,r^*}{c_p\,\Delta T}\right)^{1/5}. \tag{13}$$

However, since $\delta_{\max}$ and $\vartheta_{\min}$ are commonly unknown, the calculation by equations (10)–(12) causes difficulties and the results obtained by (13) can be uncertain.

Further studies on condensation inside cylindrical tubes are associated with the development of rotating heat pipes [21, 25–31]. In these devices, vapour is supplied from the evaporator and is completely condensed in the cooler (condenser), the liquid formed returning to the evaporator. The authors [25–30] have elaborated on the procedures for calculating heat transfer and condensate distribution along the heat pipe under the condition of a constant heat flux through the condensation surface and with the assumptions made in the Nusselt analysis. The assumption that the condensate film thickness is essentially less than the tube radius ($\delta \ll R$) has allowed the problem to be considered in Cartesian coordinates. Nevertheless, the formulae are tedious, and no recommendations on their application are given in these works.

The most complete statement (in cylindrical coordinates, with regard to liquid and vapour flow interaction (Fig. 5b)) to the problem of heat and mass transfer in a cylindrical condenser of a rotating heat pipe is solved in [31]. To calculate liquid film thickness along the condenser,

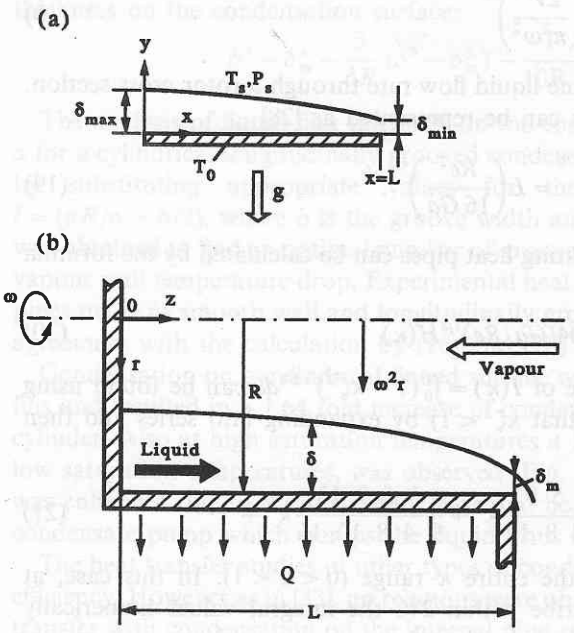

Fig. 5.

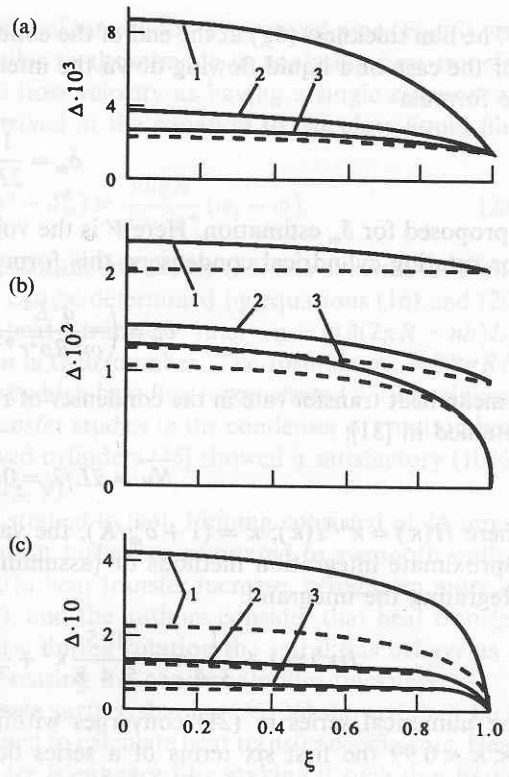

Fig. 6.

expressions are derived whose dimensionless form ($\Delta = \delta/R, \zeta = z/L$) is:

$$\Delta^4 - \Delta_m^4 - \tfrac{8}{5}(\Delta^5 - \Delta_m^5) + \tfrac{2}{3}(\Delta^6 - \Delta_m^6) = \tfrac{3}{2}D(1-\zeta^2) \tag{14}$$

without interaction between liquid and vapour and

$$\Delta^2 - \Delta_m^2 - E\ln[(\Delta^2 + E)/(\Delta_m^2 + E)] = \frac{3D}{4E}(1-\zeta^2), \tag{15}$$

with regard to such an interaction (a shear stress at the liquid–vapour interface was specified in the form $S_s = -(j_n w + f_v \rho w^2/8)$ where the first term describes the resistance due to vapour flow momentum on account of condensation and the second, due to viscous molecular forces). The complex $D = L/R)^4 Re/Ga$ $(Ga = \omega^2 RL^3/\nu^2$, $Re = 4G_1/\nu = 4qL/(\nu\rho r^*)$, G_1 is the volume liquid flow rate per unit pipe cross section length at the end of the condenser), allows for the effect of construction parameters and operating conditions; the complex $E = [4\nu/\nu_v + R\rho Re/(4\rho_v L)]^{-1}$ includes interaction at the interface. In Fig. 6, liquid distribution profiles along the condenser are given for different condensation conditions.

Based on the analysis of calculations by equations (14) and (15) with $D < 0.001$ and $E^2 > D$, the authors of [31] recommend calculating liquid film thickness on the condensation surface by the formula:

$$\Delta^4 - \Delta_m^4 = \tfrac{3}{2}D(1-\zeta^2) \tag{16}$$

or

$$\delta = \left[\frac{6\mu q}{\rho^2\omega^2 R r^*}(L^2 - z^2) + \delta_m^4\right]^{1/4}, \tag{17}$$

where $K = 6\mu q L^2/(\rho^2\omega^2 R\, r^*) = 1.5\, Re/Ga$.

The film thickness (δ_m) at the end of the condenser depends on particular liquid flow conditions. For the case of a liquid flowing down the internal surface of a rotating extended cylinder, in [32] the formula

$$\delta_m = \frac{1}{2R}\left(\frac{2V^2}{\pi^2\omega^2}\right)^{1/3} \tag{18}$$

is proposed for δ_m estimation. Here V is the volume liquid flow rate through a rotor cross section. For rotating cylindrical condensers, this formula can be represented as [28]

$$\delta_m = \left(\frac{q^2L^2}{\omega^2R\rho^2r^{*2}}\right)^{1/3} = L\left(\frac{Re^2}{16\,Ga}\right)^{1/3}. \tag{19}$$

A mean heat transfer rate in the condenser of rotating heat pipes can be calculated by the formula obtained in [31]:

$$\overline{Nu} = \bar{\alpha}L/\lambda = 0.904(Ga/Re)^{1/4}H(\kappa) \tag{20}$$

where $H(\kappa) = \kappa^{1/4}I(\kappa)$; $\kappa = (1 + \delta_m^4/K)$, the value of $I(\kappa) = \int_0^1 (1 - \kappa\zeta^2)^{-1/4}d\zeta$ can be found using approximate integration methods or (assuming that $\kappa\zeta^2 < 1$) by expanding into series and then integrating the integrand:

$$I(\kappa) = 1 + \frac{1}{3\ 4}\kappa + \frac{1\ 5}{5\ 4\ 8}\kappa^2 + \frac{1\ 5\ 9}{7\ 4\ 8\ 12}\kappa^3 + \frac{1\ 5\ 9\ 13}{9\ 4\ 8\ 12\ 16}\kappa^4 + \cdots \tag{21}$$

The numerical series in (21) converges within the entire κ range ($0 < \kappa < 1$). In this case, at $0 < \kappa < 0.99$ the first six terms of a series describe within 2% the integral values numerically obtained on a computer. In Fig. 7, $I(\kappa)$ and $H(\kappa)$ are plotted.

The estimation of the δ_m effect on the heat transfer rate [31] has shown that at $Re < 100$ the error which appears if $\delta_m = 0$ does not exceed 10%.

In a number of studies [28–31, 33, 34] the methods of heat transfer enhancement with vapour condensation in rotating horizontal cylindrical pipes by surface profiling are considered. The most simple and well-developed technique of profiling an internal tube surface is by longitudinal grooving. In the presence of grooves the condensate bulk flows across rather than along the surface, then flows down into the grooves and moves through beyond the evaporator. This decreases the flow rate through the film cross section and, consequently, its thickness. In the grooves condensate is caused to flow both by the pressure gradient along the groove and by the constituent centrifugal force (recessing grooves). This allows the grooves to be made large with a low hydraulic resistance. This provides effective condensate removal at high heat loads.

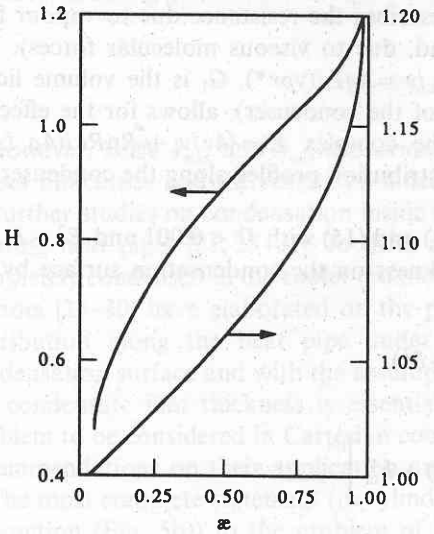

Fig. 7.

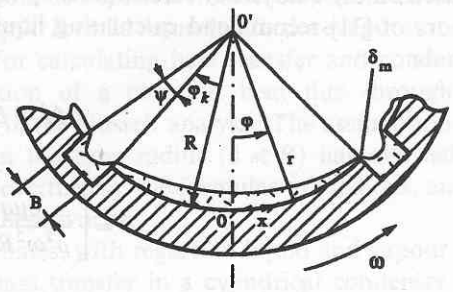

Fig. 8.

Heat transfer with vapour condensation in a cylindrical longitudinally grooved pipe (Fig. 8) was discussed in refs [28–31]. With the assumptions similar to those made in analysing heat transfer in cylindrical condensers as well as assuming liquid flow velocity as having a single component, φ, along the coordinate (Fig. 8); $\omega^2 R \gg 2v\omega$, we arrived at the equation to calculate liquid film thickness on the condensation surface:

$$\delta^4 - \delta_m^4 - \frac{3}{5R}(\delta^5 - \delta_m^5) - \frac{1}{10R^2}(\delta^6 - \delta_m^6) = \frac{6\mu q R}{\rho^2 \omega^2 r^*}(\varphi_k - \varphi). \tag{22}$$

The analysis of liquid film thickness on the condensation surface by (22) has shown that δ and α for a cylindrical longitudinally grooved condenser can be determined by equations (16) and (20) by substituting appropriate values for the heat transfer rate: $q = Q/[(2\pi R - nb)L]$, $l = (\pi R/n - b/2)$, where b is the groove width and n is their number. The formula $n_{op} = 0.8\pi R/b$ was obtained to find an optimal number of grooves at which heat flux is transferred with a minimal vapour wall temperature drop. Experimental heat transfer studies in the condenser of rotating heat pipes made as smooth wall and longitudinally grooved cylinders [35] showed a satisfactory (10%) agreement with the calculation by (16) and (20) (Fig. 9).

Condensation on a cylindrical finned surface was studied in [33]. Finning consisted of 16 screw fins and resulted in a 1.64 fold increase of condensation surface as compared to a smooth walled cylinder. Also at high saturation temperatures a 100% heat transfer increase, being even more at low saturation temperatures, was observed (Fig. 10), and the authors consider that heat transfer was enhanced due to the surface increase and because during rotation the spiral fins behave as a condensate pump which pumps the liquid, thus decreasing the condensate film thickness.

The heat transfer studies of other types of condensate surface shaping [35, 36] showed their high efficiency. However as in [33], no relations were obtained to calculate heat transfer coefficients. Heat transfer with condensation on the internal pipe surface is enhanced by making it such that liquid flow is induced by a pressure gradient along the film and by a constituent centrifugal force (conical, parabolloid and other surfaces). The greatest number of works [24, 29, 33, 36, 37, 39, etc.] are devoted to condensation studies on conical surfaces.

Laminar film condensation on the internal surface of rotating truncated cones (Fig. 11) was considered in [24] with all Nusselt theory assumptions made. An expression was derived for the condensate mass velocity through the cone cross-section:

$$G = \frac{2\pi\rho^2\omega^2}{\mu}\cos\varphi\left\{(R_0 + x\sin\varphi - \delta\cos\varphi)\left(tg\varphi - \frac{d\delta}{dx}\right)\left[\frac{\delta^3}{3}(R_0 + x\sin\varphi) - \tfrac{5}{24}\delta^4\cos\varphi\right]\right\}. \tag{23}$$

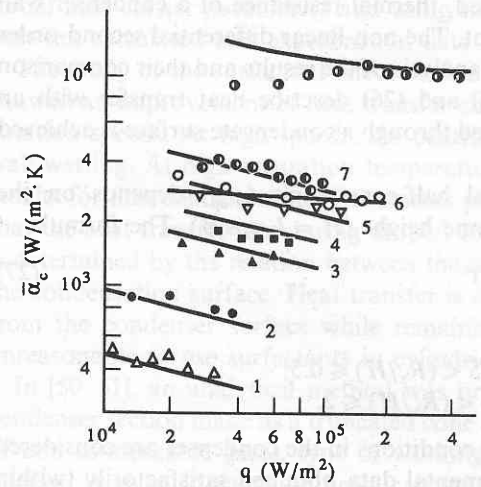

Fig. 9.

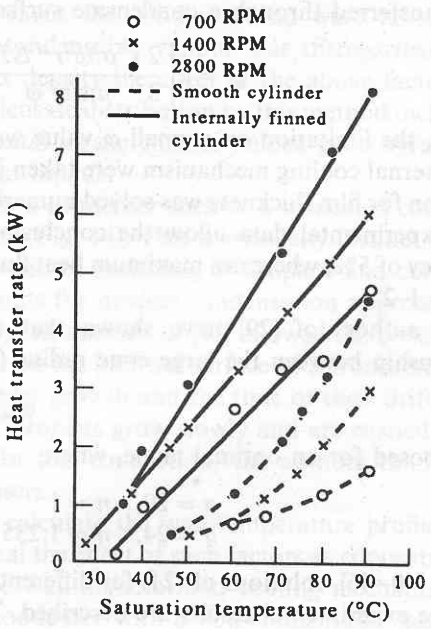

Fig. 10.

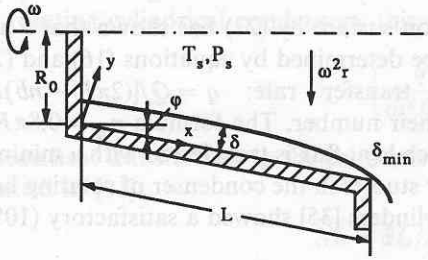

Fig. 11.

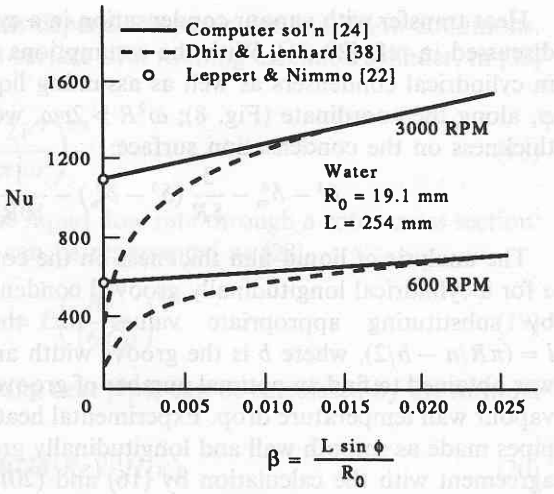

Fig. 12.

Substituting (23) into the energy balance equation for a condensate element δ high and dx long:

$$\frac{dQ}{dx} = r^* \frac{dG}{dx} \tag{24}$$

a differential equation of the second order for the film thickness can be obtained, The results of numerical solution of (24) at $\varphi = 0$ well agree with the solution by (13) [22] (Fig. 12). For $\varphi > 0$, even at very small (almost zero) half-cone angles, the mean Nusselt number exactly agrees with the solution [38] at $\beta > 0.025$ as applied to the case of rotating truncated cones:

$$Nu = 0.904\left(\frac{\omega^2 L^2 R_0^2}{\nu^2}\frac{Pr\, r^*}{c_p \Delta T}\right)^{1/4} B(\beta), \tag{25}$$

where

$$B(\beta) = \frac{[(1+\beta)^{8/3} - 1]^{4/3}}{\beta^{1/2}(2+\beta)}, \quad \beta = \frac{L \sin\varphi}{R_0}.$$

In [37], equation (24) was solved for $tg\varphi \gg (d\delta/dx)$. An expression was obtained for the heat flux transferred through a condensate surface:

$$Q = \pi\left[\frac{2}{3}\frac{\lambda^3 \rho^2 \omega^2 r^* \Delta T}{\mu \sin^2\varphi}\right]^{1/4} [(R_0 + L\sin\varphi)^{8/3} - R_0^{8/3}]^{3/4}. \tag{26}$$

In [39], the limitation on a small φ value was eliminated, thermal resistance of a condenser wall and external cooling mechanism were taken into account. The non-linear differential second-order equation for film thickness was solved numerically. The analysis of the results and their comparison with experimental data allow the conclusion that (25) and (26) describe heat transfer with an accuracy of 5%, whereas a maximum heat flux transferred through a condensate surface is achieved at $\varphi = 1$–$2°$.

The authors of [29] have shown that the optimal half-cone angle (φ_{op}) depends on the relationship between the large cone radius (R_h) and cone height ($H = L\cos\varphi$). The formula

$$\varphi_{op} = a(R_h/H)^n \tag{27}$$

is proposed for an optimal angle, where

$$a = 20, \quad n = 1 \quad \text{for} \quad 0.05 < (R_h/H) \leqslant 0.5;$$
$$a = 24, \quad n = 1.235 \quad \text{for} \quad 0.5 < (R_h/H) \leqslant 2.$$

In refs [40–46], solutions of (24) for different boundary conditions in the condenser are considered and the experimental results are described. The experimental data obtained satisfactorily (within 20%) agree with theoretical predictions.

In addition to the main forces affecting a condensate layer, the forces of vapour friction against the interface were taken into account [47, 48] as well as the resistance moment induced by the inert mass of condensable vapour supplied to the film. In so doing a shear stress at the interface was expressed as a sum of friction stress and that of the resistance moment due to the inert mass of condensable vapour. Assuming the centrifugal acceleration to be constant over the entire condenser length and equal to $\omega^2\bar{R}$, where $\bar{R}$ is the mean surface radius, the expression for heat transfer was derived:

$$Nu = \frac{\alpha L}{\lambda} = \tfrac{4}{3} Sh_L \left(\frac{\delta_L}{L}\right)^3 - \tfrac{1}{2} Dr_L \left(\frac{\delta_L}{L}\right)^2 - \tfrac{1}{2} Re_{vL} \left(\frac{\delta_L}{L}\right), \tag{28}$$

where

$$Sh_L = \frac{\rho^2(\omega^2\bar{R} - g_0) r^* x^3 \sin\varphi}{4\mu\lambda\,\Delta T}, \tag{29}$$

$$Dr_L = \frac{\rho\tau_v r^* x^2 \cos\varphi}{\mu\lambda\,\Delta T}, \tag{30}$$

$$Re_{vL} = \frac{\rho w_v x \cos\varphi}{\mu}. \tag{31}$$

The analysis of the results of numerical calculations by (28) showed that for moderate heat loads (up to $1 \times 10^5\ \mathrm{W\,m^{-2}}$) the effect of the foregoing forces is negligible and can be disregarded in practice. The authors' experimental studies on Freon-113 condensation have proved the reliability of the calculation procedure.

If the vapour–liquid interface friction is negligible, then (28) is of the form

$$Nu = \tfrac{4}{3} Sh_L \left(\frac{\delta_L}{L}\right)^3 \tag{32}$$

or, allowing for (29)

$$Nu = 0.943 \left(\frac{\omega^2\bar{R}^2 L^2}{\nu^2} \frac{Pr\, r^*}{c_p\,\Delta T}\right)^{1/4} \beta^{1/4}, \tag{33}$$

where $\beta = L \sin\varphi / R_0$.

At small β, the results of calculations by (32) agree well with the calculations by (25) and (26).

In [49], the vapour pressure gradient due to friction, vapour velocity reduction during condensation and vapour cross section decrease towards the condenser end were taken into account. However, the effect of the inert mass of condensable vapour was disregarded. The calculations have shown that even at a high heat flux density the effect of the above factors on heat transfer is negligible (Fig. 13). Calculation of condensate distribution by this method including initial heat carrier parameters and using the experimental measurements yielded good agreement between calculated and experimental data for different liquids.

The study of the surfactant effect on heat transfer in a condenser such as a truncated cone [33] showed an improvement of heat transfer characteristics (Fig. 14). This is especially distinct at low rotation speeds. At high speeds, the centrifugal force causes flattening of droplets and complete wall wetting. At high saturation temperatures, the results for droplet condensation approach the results for film condensation. The studies performed by the authors of [33] allowed the conclusion that the heat transfer rate during droplet condensation on the internal surface of a truncated cone is determined by the relation between the time of droplet growth and the time of their drift from the condensation surface. Heat transfer is enhanced if droplets grow slowly and are carried away from the condenser surface while remaining small. In this connection, the authors think it is unreasonable to use surfactants in cylindrical condensers.

In [50–51], an analytical method was proposed to calculate the wall temperature profile of a condenser section made as a truncated cone and to reveal the effect of such factors as concentration of non-condensable gases, type of working fluid, pipe wall material and cooling mechanism. A relation is given to calculate heat transfer from the condenser with a non-condensable gas. The computer calculations made by the proposed methods agree satisfactorily with experimental data.

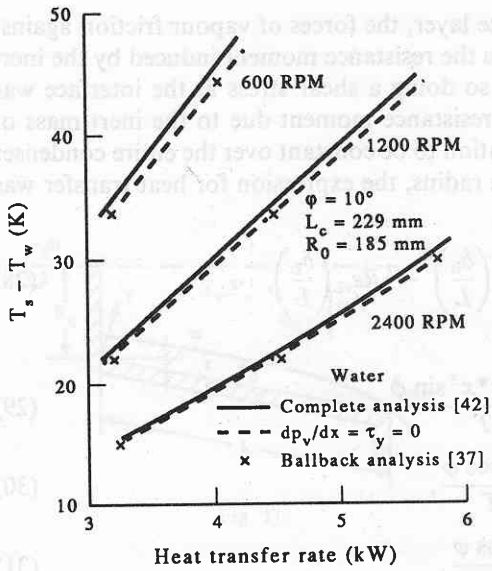

Fig. 13.

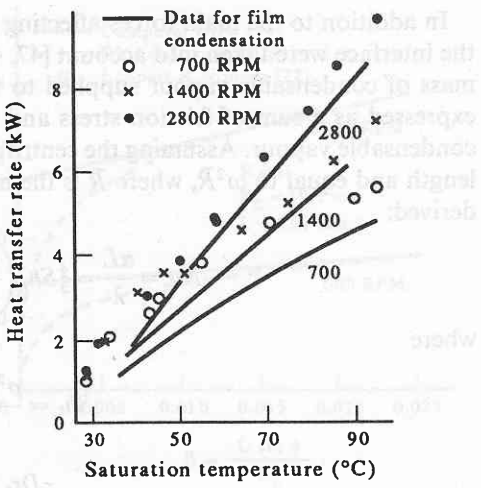

Fig. 14.

The heat transfer rate during vapour condensation in rotating pipes can be enhanced essentially when the condensation surface is a regular polygonal prism with longitudinal grooves in its angles (Fig. 15), as in this case the condensate will move under the action of the constituent centrifugal force. The authors of [31] have considered laminar film condensation of immovable vapour in the condenser as a regular polygonal prism. The formula $\delta = [3\mu q/(\rho^2\omega^2 r^*)]^{1/3}$ (a film thickness is constant) has been derived to calculate liquid film thickness on the condensation surface. The following expression is proposed to calculate temperature drop in the condenser of a regular n-angular prism with the circumferential radius (R), length (L) and width of grooves (b):

$$\Delta T = \left(\frac{3\mu}{\rho^2\omega^2\lambda^3 r^*}\right)^{1/3}\left\{\frac{Q}{2nL}\left[R\sin\frac{\pi}{n} - b\Big/\left(2\cos\frac{\pi}{n}\right)\right]^{-1}\right\}^{4/3} \tag{34}$$

The analysis of (34) shows that the optimal number of prism walls for which the temperature drop is minimal ranges between 6 and 8. In Fig. 16 temperature drop in different condensers is plotted as a function of heat flux transferred through them. The geometrical condenser parameters (length, diameter and width of grooves) and the rotation speed were equal, water being used as a heat carrier. As seen from the figure, longitudinal grooves on a cylindrical surface essentially reduce temperature drop, which can be much less than in conical condensers. The internal condenser surface made as a regular polygonal prism leads to 2–3 fold reduction of the temperature drop as compared to the condenser as a longitudinally grooved cylinder.

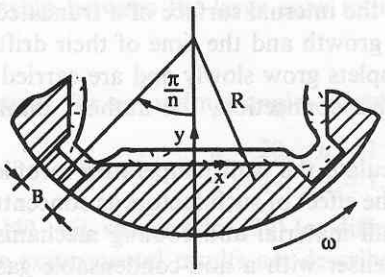

Fig. 15.

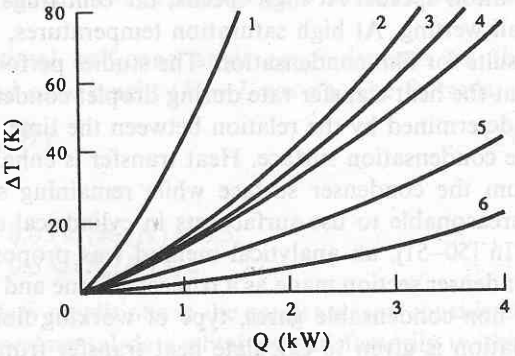

Fig. 16.

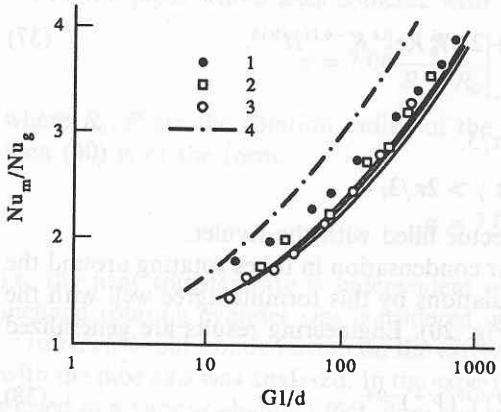

Fig. 17.

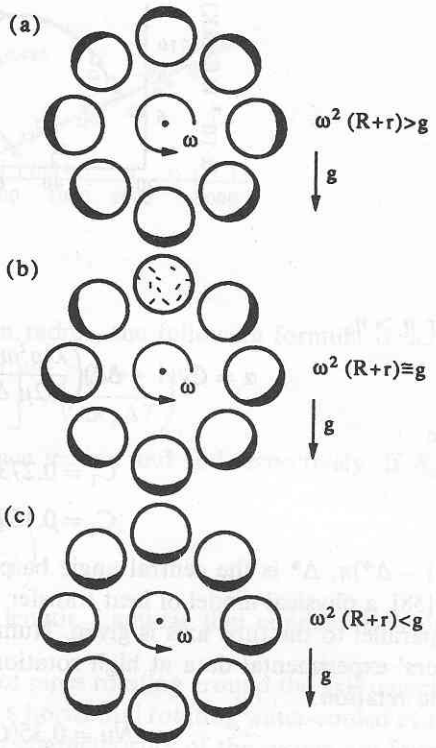

Fig. 18.

3.2. *Condensation in tube rotating around the axis which does not coincide with the tube symmetry axis*

Vapour condensation in tubes rotating around the axis which do not coincide with the tube axis is used to develop the air-cooled condensers, heat pipe cooled electric machines [52, 53], etc. The effect of centrifugal forces on heat transfer with vapour condensation inside a vertical tube rotating around the axis parallel to the tube axis has been studied experimentally and theoretically in ref. [54].

A physical model is proposed which includes the region of a condensate flow. The investigation results (Fig. 17) have shown that the total heat transfer coefficient essentially increases with centrifugal acceleration, and its value proves to be somewhat lower as compared to condensation on the external surface of a circular tube (see ref. [59]) with the same field of centrifugal forces.

Flow dynamics in a tube rotating around the horizontal axis parallel to the tube axis, or inclined at some angles to it, was studied in refs [55–58, 60, 61]. An intricate nature of liquid flow is found. It is determined by the relation of centrifugal and gravity forces and the physical properties and quantity of the liquid (Fig. 18). At low rotation frequencies, the liquid uniformly flows around the entire internal surface as a rivulet (Fig. 18c) or vibrates relative to the tube generatrix mostly remote from the rotation axis (Fig. 18b). The analysis of experimental data yielded [60] the formula to determine the critical rotation frequency at which transition between liquid flow patterns occurs:

$$\eta_{cr} = 0.53\,(R^*)^{0.23} Re^{0.06} H^{0.08}. \tag{35}$$

It is valid for $Re = \omega R_t\, h/\nu = 6 \ldots 300$, $R^* = R_r/R_t = 4 \ldots 16$, $H = h/R_t = 0.11 \ldots 0.5$ (h is the rivulet depth).

The influence of the rotational frequency on heat transfer is shown in Fig. 19. In calculating heat transfer with condensation, the following relation is obtained for $\eta < \eta_{cr}$

$$Nu = \alpha h/\lambda = 535 Re^{-0.25} K^{-0.3}, \tag{36}$$

where $Re = 30 \ldots 2200$, $K = q l_t/(\rho r^* \nu)$.

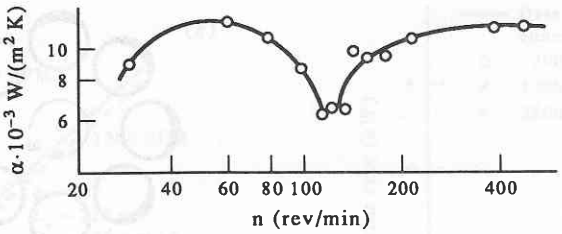

Fig. 19.

For $\eta > \eta_{cr}$

$$\alpha = C_T(1-\Delta^*)\left(\frac{\lambda^3\rho^2\omega^2 R_R r^*}{2\mu\,\Delta T R_t}\right)^{1/4} + 2.07\frac{\lambda}{h}Re_h^{0.4}K^{-0.15}H^{0.18}, \tag{37}$$

where

$$C_T = 0.273\gamma \text{ at } \gamma \leqslant 2\pi/3,$$

$$C_T = 0.159\gamma + 0.25 \text{ at } \gamma > 2\pi/3,$$

$\gamma = (1-\Delta^*)\pi$, Δ^* is the central angle based on the sector filled with the rivulet.

In [58], a physical model of heat transfer with vapour condensation in tubes rotating around the axis parallel to the tube axis is given. Numerical calculations by this formula agree well with the authors' experimental data at high rotation speeds (Fig. 20). Engineering results are generalized by the relation

$$Nu = 0.35(Ga\,Pr\,G^*/H)^{0.25}(V^+)^{-0.4}, \tag{38}$$

where V^+ is the amount of tube filled with liquid, %; $G^* = \eta = a/g$, $H = c\rho\Delta T/r^*$.

4. CONDENSATION ON AN EXTERNAL ROTATING TUBE SURFACE

Condensation with a laminar film flow and immovable vapour was studied in ref. [62]. Experiments have shown that the heat transfer coefficient depends on the rotation speed and may achieve the values encountered in dropwise vapour condensation. Condensate thrown from the pipe surface by the centrifugal force accounts for α increase in the case of a rotating heat transfer surface.

For the rotating pipes whose axis is parallel to the rotation axis, the heat transfer coefficient is determined by the formula:

$$\alpha = 0.876\frac{\lambda}{d}\left(\frac{d^3\omega^2 R_R r^*}{vac_p\,\Delta T}\right)^{1/4}, \tag{39}$$

where d is the external tube diameter and R_R is the rotation radius.

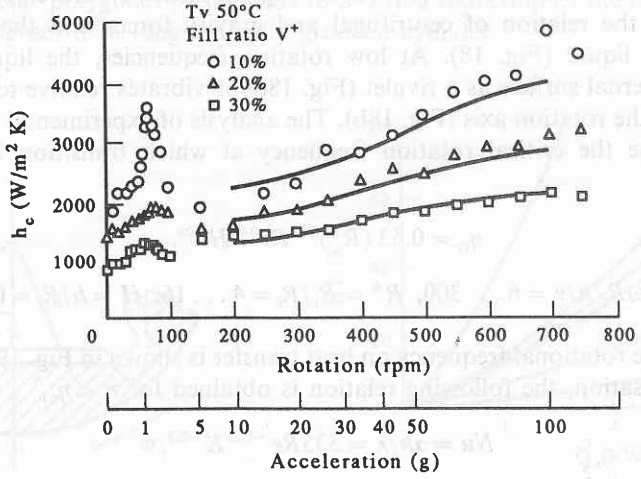

Fig. 20.

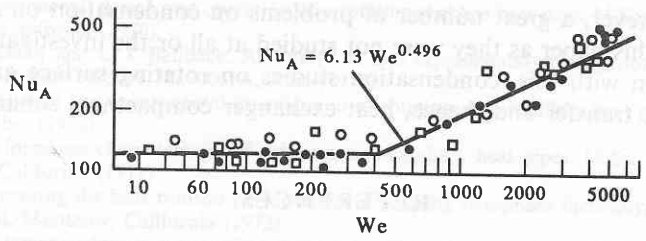

Fig. 21.

For the pipes whose axes coincide with the rotation radius, the following formula is derived:

$$\alpha = 7.06 \frac{R}{R - R_0}\left[1 - \left(\frac{R_0}{R}\right)^{4/3}\right]^{3/4} \lambda \left(\frac{\omega^2 r^* }{v a c_p \Delta T}\right)^{1/4} \tag{40}$$

where R_0, R are the rotation radius of the pipe entrance section and end respectively. If $R_0 = 0$, then (40) is of the form:

$$\alpha = 7.06 \lambda \left(\frac{\omega^2 r^*}{v a c_p \Delta T}\right)^{1/4}, \tag{41}$$

i.e. the heat transfer rate is independent of the tube length. Laminar film condensation on an inclined rotating cylinder was considered in [63].

In refs [64–66], condensation on the external surface of pipes rotating around the axis coinciding with the pipe axis was analysed. In the experiments with a horizontal rotating water-cooled cylinder placed in a vapour chamber [64], flow and heat transfer characteristics of the system are found to pass through three stages. At low rotation speeds, the centrifugal force and the friction force between the cylinder and condensate film tend to counteract the gravity force which in some cases results in condensate film retention on the cylinder and in a heat transfer decrease. Higher rotation speeds correspond to the second phase when liquid is pulverized, film thickness diminishes and heat transfer increases, At high rotation speeds, the film becomes very thin and droplets appear which grow to become convective plumes. Within this last stage, the heat transfer rate gradually decreases. The authors have proposed physical models and theoretical estimates for heat transfer for two of these regimes. They showed that at large rotation speeds, the equation $Nu = f\,We^{0.5}$ should hold.

The studies of the diameter and rotation speed effect on heat transfer with condensation on horizontal water-cooled cylinders [65] showed the presence of a condensate film throughout a laminar flow. No heat transfer coefficient variation was observed in a wide Weber number range.

Heat transfer with vapour condensation on a vertical pipe rotating around its axis was experimentally studied in [66]. As shown, the heat transfer coefficient grows with the rotation speed, and for its high values is 4–5 times higher. The results related to the Nusselt and Weber numbers show that for the Weber numbers less than 500, the Nusselt number is constant, whereas for Weber numbers more than 500, the correlation equation:

$$Nu_A = 6.13\ We^{0.496} \tag{42}$$

is valid.

In Fig. 21, experimental data are compared with relation (42). At high rotation speeds ($We > 500$) this relationship describes well the experimental results for horizontal cyliners [65].

The results of experimental heat transfer studies with condensation on a horizontal rotating cylinder [29, 67] showed the validity of the relationship between the Nusselt and Weber numbers proposed in ref. [65]. The authors emphasized the effect of cylinder surface finish on heat transfer rate.

5. CONCLUSION

The materials of this short review prove the possibility of essential condensation enhancement by rotating a cooling surface. The calculation formulae and relationships given in this work offer heat transfer rates with vapour condensation on some surface types and can be used for developing

heat exchangers. However, a great number of problems on condensation on rotating bodies are beyond the scope of this paper as they were not studied at all or the investigation range was very narrow. In connection with this, condensation studies on rotating surface are timely, their use resulting in high heat transfer and, hence, heat exchanger compactness enhancement.

REFERENCES

1. K. C. D. Hickman, Centrifugal boiler compression still. *Ind. Engng Chem.* **49,** 786 (1957).
2. R. U. Clark and L. A. Bromley, Saline water conversion by multiple-effect rotating evaporator. *Chem. Eng. Prog.* **57,** 64 (1961).
3. E. M. Sparrow and J. L. Gregg, A theory of rotating condensation. *J. Heat Transfer, Trans. ASME*, Series C **81,** 113–120 (1959).
4. W. Nusselt, Die Oberflachenkondensation des Wasserdampfes. *Zeitschrift VDL* **60,** 541–546, 568–575 (1916).
5. Ju. G. Gulev, *Trans. CKTI*, No. 57 (1965).
6. V. B. Astafiev, *Experimental of condensations transfer on rotating disk*. Cand. thesis. MEI Moscow (1968).
7. V. H. Rifert, Experimental Investigation of Heat Transfer for Distill on Rotating Disk. Cand. thesis. KPI, Kiev (1969).
8. S. S. Nandapurkar and K. O. Beatty, *Chem. Eng. Prog.* **56,** No. 30 (1960).
9. V. B. Astafiev and A. M. Baklastov, Vapor condensation on rotating horizontal disc. *Teploenergetika* **9,** 55–57 (1970).
10. A. I. Butuzov, V. H. Rifert, Experimental investigation of heat transfer with vapor condensation on rotating disk. *Energetica* **2,** (1969).
11. L. A. Bromley, R. F. Humphreys and W. Murray, Condensation on and evaporation from radially grooved rotating disks. *J. Heat Transfer, Trans. ASME*, Series C **86,** (1965).
12. L. I. Archipov and A. M. Baklastov, Experimental investigation of heat and mass transfer with vapor condensation on rotating disk from vapor–air. *Teploenergetika* **9,** 83–84 (1971).
13. P. A. Juchkov, *Process of Drying in Paper Production*. Lesnaja promishlennost, 140p., (1965).
14. H. P. Greenspan, On a rotational flow disturbed by gravity. *J. Fluid Mech.* **72**(2), 335–351 (1976).
15. K. J. Ruchak and L. E. Scriven, Rimming flow of liquid in a rotating horizontal cylinder. *J. Fluid Mech.* **76**(1), 113–125 (1976).
16. R. F. Gans, On steady flow in a partially filled rotating cylinder. *J. Fluid Mech.* **83**(3), 415–427 (1977).
17. J. A. Deiber and R. L. Cerro, Viscous flow with a free surface inside a horizontal rotating drum. 1 Hydrodynamics. *Ind. Engng Chem. Fundam.* **15**(2), 102–110 (1976).
18. M. G. Semena and Ju. A. Chmelev, Study of liquid hydrodynamics regimes in a smooth-wall rotating heat pipe. *J. Engng Physics* **23,** 766–774 (1982), **24,** 8–14 (1983).
19. W. Nakayama, Y. Ohtsuka, H. Itoh and T. Joshikawa, Optimum charge of working fluids in horizontal rotating heat pipes. In *Proc. Int. Conf. Heat and Mass Transfer in Rotating Machinery*, Dubrovnik (1982).
20. M. P. Kukharsky, B. N. Krivosheev and V. V. Khrolenok, Of heat transfer in centrifugal heat pipes. *Design and Cooling of Special Electric Machines in Technology*. pp. 61–70. Kharkov (1987).
21. J. A. Khmelev, Heat Transfer and Hydrodynamics in Cylindrical Rotating Heat Pipes. Cand. thesis, p. 238 ITTF, Kiev (1984).
22. G. Leppert and B. Nimmo, Laminar film condensation on surface normal to body and inertial forces. *J. Heat Transfer* **90,** 178–179 (1968).
23. B. Nimmo and G. Leppert, Laminar film condensation on a finite horizontal surface. *Heat Transfer 1970, V. G.*, Elsevier, Amsterdam (1970).
24. P. I. Marto, Lamar film condensation on the inside of slender, rotating truncated cones. *J. Heat Transfer* **95,** 270–272 (1973).
25. M. P. Kukharsky, B. N. Krivosheev and A. A. Firsanov, Method of calculation of condensate allocation in cylindrical centrifugal heat pipes. *Aerodynamics and Heat Transfer in Electric Machines*, pp. 64–68. KhAI Press, Kharkov (1976).
26. B. N. Krivosheev, M. P. Kukharsky and V. D. Portnov, Investigation of heat transfer in centrifugal heat pipes with optimum layer of liquid. *Trans. MEI* No. 448, 32–35 (1980).
27. M. Bubenicek, Vypocet a Moznostu Intensifikace Rotachnich Horizontalnich Tepelnych Trubic. Sb: Tepelni Trubice a Jejich Apllikace pouziti v Prumyslu. s. 118–125, Praha (1977).
28. L. L. Vasiliev and V. V. Khrolenok, Study of heat transfer process in the condensation zone of rotating heat pipes. *J. Heat Recovery Systems* **3,** 281–290 (1983).
29. L. L. Vasiliev, S. V. Konev and V. V. Khrolenok, *Heat Transfer Enhancement in Heat Pipes*. Nauka i Tekhnika, Minsk (1986).
30. L. L. Vasiliev, V. Kalita and V. V. Khrolenok, Heat transfer enhancement in the centrifugal heat pipe condenser. *J. Engng Physics* **46,** 538–545 (1984).
31. L. L. Vasiliev, V. V. Khrolenok, *Heat and Mass Transfer in Centrifugal Heat Pipes*, (Preprint 42). HMTI, Minsk (1987).
32. V. I. Sokolov, *Centrifugaling*, Chemistry, Moscow (1976).
33. P. J. Marto and L. L. Wagenseil, Augmenting the condenser heat-transfer performance of rotating heat pipes. *AIAA*. **17,** 647–652 (1979).
34. P. J. Marto and H. Weigel, The development of economical rotating heat pipes. In *Advances in Heat Pipe Technology*, D. A. Reay (ed.), pp. 709–723. Pergamon Press, Oxford (1981).
35. V. V. Khrolenok, *Heat and Mass Transfer in Centrifugal Rotating Heat Pipes by Height Frequency*. Cand. thesis, p. 210. HMTI Minsk (1985).
36. P. J. Marto, Rotating heat pipes. In *Proc. Int. Conf. Heat and Mass Transfer in Rotating Machinery*, Dubrovnik (1982).
37. L. J. Ballback, The operation of a rotating, wickless heat pipe. M.Sc. thesis, Naval Postgraduate School, Monterey, California (1969).
38. V. Dhir, J. Lienhard, Laminar film condensation on plane and axisymmetric bodies in nonuniform gravity. *J. Heat Transfer* **93,** 97–100 (1971).

39. T. J. Daley, The experimental design and operation of a rotating wickless heat pipe. M.Sc. thesis, Naval Postgraduate School, Monterey, California (1970).
40. P. J. Marto, T. J. Daley and L. J. Ballback, An analytical and experimental investigation of rotating, non-capillary heat pipes. Annual Report NPS-59 Mx70061A, June (1970).
41. P. J. Marto, An analytical and experimental investigation of rotating, non-capillary heat pipes. Final Report NPS-59 Mx72111A, November (1972).
42. W. H. Newton, Performance characteristics of rotating, non-capillary heat pipes. M.Sc. thesis, Naval Postgraduate School, Monterey, California (1971).
43. C. E. Schafer, Augmenting the heat transfer performance of rotating two-phase thermosyphons. M.Sc. thesis, Naval Postgraduate School, Monterey, California (1972).
44. K. S. Tucker, Heat transfer characteristics of a rotating two-phase thermosyphon. M.Sc. thesis, Naval Postgraduate School, Monterey, California (1974).
45. J. S. Noodard, The operation of rotating, non-capillary heat pipes. M.Sc. thesis, Naval Postgraduate School, Monterey, California (1972).
46. P. J. Marto, Performance characteristics of rotating, wickless heat pipes. In *Proc. IInd Int. Heat Pipe Conf.*, Bologna, Italy, pp. 281–291 (1976).
47. T. C. Daniels and F. K. Al-Jumaily, Theoretical and experimental analysis of a rotating wickless heat pipe. In *Proc. Ist. Int. Heat Pipe Conf.*, Stuttgart, pp. 1–12 (1973).
48. T. C. Daniels and F. K. Al-Jumaily, Investigations of the factors affecting the performance of a rotating heat pipe. *Int. J. Heat Mass Transfer* **18,** 961–973 (1975).
49. P. J. Marto, Performance characteristics of rotating, wickless heat pipes. In *Proc. Ist Int. Heat Pipe Conf.*, Stuttgart, pp. 281–291 (1973).
50. T. C. Daniel and R. J. Williams, The effect of external boundary conditions on condensation heat transfer in rotating heat pipes. *Int. J. Heat Mass Transfer* **22,** 1237–1241 (1979).
51. T. C. Daniels and N. S. Al-Baharnah, Temperature and heat load distribution in rotating heat pipes. *AIAA J.* **18,** 202–207 (1980).
52. J. Schneller, B. Pokorny and F. Polasek, Heat transfer in rotating co-axial and parallel heat pipes and their application in machinery. *Heat and Mass Transfer Rotating Machinery*, pp. 669–688. Berlin/Washington (1984).
53. J. Niekawa and K. Matsnmoto, Performance of revolving heat pipe and application to a rotary heat exchanger. In *Proc. 4th Int. Heat Pipe Conf.*, Palo-Alto, U.S.A., pp. 225–234 (1981)
54. S. Mochizuki and T. Shiratori, Condensation heat transfer within a circular tube under centrifugal acceleration field. *J. Heat Transfer* **102,** 179–185 (1980).
55. R. Curtila and T. Chataig, Experimental study of a revolving heat pipe. In *Proc. 5th Int. Heat Pipe Conf.*, Tsukuba, Japan, p. 273 (1984).
56. A. Bontems, C. Coubier, C. Margnet, I. C. Solecki and R. Curtila, Theoretical analysis of a revolving heat-pipe. In *Proc. 5th Int. Heat Pipe Conf.*, Tsukuba, Japan, pp. 274–279 (1984).
57. J. A. Khmelev, E. V. Shevel, Investigation of hydrodynamic and heat transfer in a revolving heat pipe. In *Convection Heat Transfer and Hydrodynamic*, pp. 136–141. Nankova Dumka, Kiev (1985).
58. K. Gi and S. Maezuwa, Heat transfer characteristics of a parallel rotating heat pipe. In *Proc. 7th Int. Heat Pipe Conf.*, Minsk, USSR (1990).
59. N. N. Suryanarayana, Condensation heat transfer under high gravity condition. In *Proc. 5th Int. Heat Transfer Conf.*, Vol. 3, pp. 279–285 September (1974).
60. E. V. Shevel, Heat transfer and hydrodynamics in a revolving heat pipe. Cand. thesis, KPI, Kiev (1988).
61. Chen Jian and Tu Chuanjing, Condenser heat transfer in inclined rotating heat pipe. In *Proc. VI. Int. Heat Pipe Conf.*, Grenoble (1982).
62. I. I. Chernobylsky and G. M. Scheglov, *Trans. Hei* **1,** Kiev (1949).
63. K. E. Hassan and M. J. Jakob, Laminar film condensation of pure saturated vapors on inclined circular cylinders. *Trans. ASME, J. Heat Transfer* **80,** 887–894 (1958).
64. R. M. Singer, G. W. Prechkshot, Condensation of vapor on a horizontal rotating cylinder. In *Proc. Heat Transfer and Fluid Mechanics Institute*, pp. 205–216 (1963).
65. R. Hoyle, D. H. Matthews, The effect of diameter, size and speed of rotation on the heat transfer from steam to cooled cylinders. *Int. J. Heat Mass Transfer* **7,** 1224–1229 (1964).
66. A. Nicol and M. Gacesa, Condensation of steam on a rotating vertical cylinder. *Trans. ASME, J. Heat Transfer* **92,** (1970).
67. L. L. Vasiliev and V. V. Khrolenok, Centrifugal coaxial heat pipes. In *Proc. IInd Int. Heat Pipe Conf.*, Bologna, Italy (1976).